



Effect of dissolved carbon dioxide on the sonocrystallisation and physical properties of anhydrous milk fat

Tuyen Truong^{a, b}, Martin Palmer^c, Nidhi Bansal^a, Bhesh Bhandari^{a, *}

^a ARC Dairy Innovation Hub, School of Agriculture and Food Sciences, The University of Queensland, Queensland, 4072, Australia

^b School of Science, RMIT University, Victoria, 3001, Australia

^c School of Engineering, University of Melbourne, Victoria, 3010, Australia

ARTICLE INFO

Article history:

Received 20 July 2018

Received in revised form

31 January 2019

Accepted 1 February 2019

Available online 22 February 2019

ABSTRACT

The effects of dissolved CO₂ (0–2000 ppm) coupled with ultrasound (US; 20 kHz) on the physical properties of anhydrous milk fat (AMF) were examined. Carbonated AMF was sonicated at 28 °C for 5 s at various amplitudes and subjected to isothermal (28 °C) and non-isothermal (cooling from 28 to 5 °C) crystallisation conditions. AMF microstructure, thermal properties and hardness were evaluated after 48 h of storage. In general, carbonated AMF samples treated with the same US amplitude exhibited a slight decrease in endset-melting temperature, smaller fat crystals with denser fat crystal network. Dissolved CO₂ caused harder texture of sonicated AMF at 25 °C. However, when carbonated + sonicated AMF samples was stored at 5 °C, their texture appeared to be softer than that of the control sample. A protective effect of CO₂ against formation of primary oxidative products during 90 days of storage was evidenced in both non-sonicated and sonicated AMF.

© 2019 Published by Elsevier Ltd.

1. Introduction

Along with lipid composition, crystallisation behaviour is one of major factors influencing the physical functionality and processability of edible fats and oils. The bulk crystallisation properties of food lipids can in turn be related to microstructural parameters (crystal size, crystal shape, and number of crystals), solid fat content and polymorphic transformation of crystal types. Various formulation, processing and conditioning approaches have been used to modulate crystallisation of edible lipids such as temperature programming (Lopez, Lavigne, Lesieur, Keller, & Ollivon, 2001), additives (Smith, Bhaggan, Talbot, & van Malssen, 2011), shear treatment (Marangoni et al., 2012), emulsification (Han et al., 2014) and sonication (Martini, Suzuki, & Hartel, 2008).

Modulation of crystallisation by ultrasound (“sonocrystallisation”) has been applied successfully to various food systems including water (Zhang, Inada, & Tezuka, 2003), lactose (Zamanipour, Dincer, Zisu, & Jayasena, 2013), edible oils (Chemat et al., 2004; Higaki, Ueno, Koyano, & Sato, 2001), shortenings (Suzuki, Lee, Padilla, & Martini, 2010), milk fat (Frydenberg,

Hammershoj, Andersen, & Wiking, 2013; Martini et al., 2008), cocoa butter (Higaki et al., 2001) and vegetables (Xu, Zhang, Bhandari, & Cheng, 2014). Subject to the precise treatment conditions used, in many of these matrices, a common effect of sonocrystallisation is to accelerate crystallisation and generate a larger number of smaller and more uniform crystals. There is particular interest in using sonocrystallisation in lipid systems, where some potentially valuable treatment effects have been demonstrated, such as the generation of sharper melting profiles and harder textures (Martini, 2013).

It has been proposed that “inertial” or “transient” cavitation is the underlying mechanism responsible for the effects of ultrasound on crystallisation of lipid molecules. In this process, unstable cavitation bubbles which are formed and imploded during sonication can serve as active sites to induce primary crystal nucleation. Expansion caused by condensation and collision of bubbles upon sonication can create shock waves, leading to formation of locally high temperature and pressure regions. Consequently, there is an increase in degree of supercooling. In addition, lipid molecules may be better aligned with high shear forces upon sonication or agitation, thereby facilitating both primary and secondary nucleation (Higaki et al., 2001; Martini, 2013). When ultrasound is applied under different conditions, it has also been shown that “stable” or “non-inertial” cavitation can

* Corresponding author. Tel.: +61 7 33469192.

E-mail address: b.bhandari@uq.edu.au (B. Bhandari).

cause remarkable changes in crystal habit and distribution. For example, different textures and improved separation efficiency during dry fractionation of anhydrous milk fat (AMF) were obtained when sonicating in the absence of transient cavitation (Arends, Blindt, Janssen, & Patrick, 2003). In fact, “non-inertial” cavitation, related to generation of stable bubbles, at relatively low intensity can induce nucleation of fat crystals (Arends et al., 2003).

In a previous study, we demonstrated that infused carbon dioxide (CO₂) can also be used to modulate crystallisation behaviour, microstructure and texture of AMF (Truong, Palmer, Bansal, & Bhandari, 2017a) and that some of these effects are similar to those seen in sonocrystallisation. That is, dissolved CO₂ enhanced crystallinity, accelerated crystal nucleation and induced a larger number of smaller crystals than observed in untreated AMF. Compared with untreated AMF, the texture of carbonated AMF was harder under isothermal crystallisation (25 °C) but softer when crystallised by rapid cooling from 35 to 5 °C. In this system, it was suggested that CO₂ molecules acted as impurities to enhance crystallisation, with CO₂ microbubbles also providing templates for heterogeneous crystal nucleation (Truong et al., 2017a).

Given these findings, it was of interest to investigate whether carbonation could be used in combination with sonication to enhance the effects of sonocrystallisation. Potential benefit of a combined treatment could extend beyond a simple synergistic effect of accelerating crystallisation. Although very little has been published on the interaction of dissolved gases and ultrasound in terms of process efficiency, at least one study suggested that higher gas contents may reduce the intensity of cavitation (Sivasankar, Paunikar, & Moholkar, 2007). This approach may help to prevent autoxidation of lipids resulting from cavitation-generated free radicals, which is a common problem in sono-processing of edible fats and oils (Chemat et al., 2004; Marchesini et al., 2012). Recently, we have demonstrated that dissolved CO₂ at 500–2000 ppm concentration is sufficient to initiate nucleation of alpha-lactose monohydrate (Adhikari, Truong, Bansal, & Bhandari, 2018; Xun, Truong, & Bhandari, 2017), leading to differences in size, shape and yield of alpha-lactose monohydrate. This effect is more pronounced when carbonation is coupled with either high power ultrasound (20 kHz) (Xun et al., 2017) or low power ultrasound (205 kHz) (Adhikari et al., 2018) as a post-mechanical treatment. From another perspective, incorporation of CO₂ into milk has been reported to reduce formation of oxidation products upon sonication treatment (Marchesini et al., 2012). CO₂ has also been found to be effective in improving oxidative stability of refined rapeseed oil (Sionek, Krygier, Ukalski, Ukalska, & Amarowicz, 2013). Indeed, gas-flushing and modified atmosphere packaging with CO₂ is used industrially for a wide range of foods to help prevent oxidative degradation, primarily by simple, displacement of dissolved and headspace oxygen.

This study investigated the combined effects of CO₂ and sonication on crystallisation and physical functionality of AMF under both isothermal and non-isothermal (cooling) crystallisation conditions. Low power, high intensity ultrasound (20 kHz frequency) was used and intensities ranging from 0.75 W cm⁻² to 45.2 W cm⁻². Crystallisation, melting properties, microstructure and hardness of AMF were analysed. As the effect of sonication on crystallisation properties of AMF has been quite thoroughly reported in the literature (Frydenberg et al., 2013; Martini et al., 2008), the work reported here is focused largely on the effects of dissolved CO₂ in sonicated samples. The possible protective effect of CO₂ against generation of primary oxidation was evaluated by measuring peroxide values (PV).

2. Materials and methods

2.1. Materials

Anhydrous milk fat (AMF; 99.9% butterfat and 0.1% moisture) was obtained from Rogers & Company Foods Pty Ltd (Hampton East, Victoria, Australia). The free fatty acid and peroxide value as per product specifications were 0.1% (as oleic acid) and below 0.01%, respectively. Analysis of fatty acid composition by gas chromatography showed that the AMF was primarily palmitic acid (C16:0; 39.40 ± 0.01%) and oleic acid (C18:1; 23.17 ± 0.03%). Unsaturated fatty acids including myristoleic (C14:1), palmitoleic (C16:1), oleic (C18:1), and linoleic (C18:2) acids accounted for 28.9% gross fatty acid composition. The AMF was kept at refrigerator temperature (4 °C) until use. Pelleted dry ice, which is the solid form of solid CO₂, was obtained from University of Queensland (Brisbane, Australia). As solid CO₂ will sublimate to gaseous CO₂ at -78.5 °C (atmospheric pressure) (Perry & Green, 2007), the dry ice was stored at -80 °C to prevent sublimation.

2.2. Dissolution of CO₂ into AMF

A home-made apparatus as described in our previous study (Truong, Palmer, Bansal, & Bhandari, 2017b) was used to dissolve CO₂ (in form of dry ice) into AMF in batch and static modes. A digital manometer (DC-400, GTS Gauges Transmitters Switches, Midvale, Western Australia) connected to a close container allowed reading of partial pressure changes during absorption of CO₂ into AMF until equilibrium state is reached (about 21–24 h). Calculation of the dissolved CO₂ concentration in AMF was based on the partial pressure reading and known amount of initial dry ice added as detailed by Truong et al. (2017b). In this study, measured CO₂ concentration is expressed as ppm by mass (mg kg⁻¹) unless otherwise specified.

2.3. Experimental procedure

AMF was completely melted at 70 °C for 1 h and cooled to 35 °C. At 35 °C, the dry ice was added into liquid AMF at three concentrations (0, 1000, and 2000 ppm) and equilibrated for 24 h in an incubator at the same temperature. Dissolution of CO₂ into AMF was monitored by changes of partial pressure reading as described above. Then liquid AMF was quickly cooled (10 °C min⁻¹) to 28 °C by immersing the container in water bath, then poured into a double-jacketed glass vessel, which was maintained at 28 °C using a circulating water bath. Sonication was applied immediately, at 20 kHz for 5 s using an ultrasound probe with a 13 mm diameter tip attached to a sonicator (Branson Digital 250, Danbury, CT, USA). Three ultrasound amplitudes (10, 30 and 50%) were examined. The combined effects of CO₂ and ultrasound on crystallisation behaviour and physical functionality of AMF were then investigated at two crystallising conditions:

- (i) AMF microstructure was observed under polarised light microscopy (PLM) for the first 75 min at 28 °C. In parallel, 40 mL of the sample was sub-divided into a plastic container and kept at room temperature (25 °C).
- (ii) Nucleation and fat crystal growth in AMF were examined during cooling from 28 to 5 °C at 0.5 °C min⁻¹. Sub-samples (40 mL each) were immediately transferred into a plastic container and maintained at refrigerated temperature (5 °C).

After 48 h storage at specific temperatures, samples were subjected to measurements of CO₂ retention, thermal properties and hardness as described in sections 2.5–2.7. To further investigate the

longer-term effect of CO₂ plus ultrasound on AMF texture, hardness was also measured after 9 days of storage.

2.4. Calculation of ultrasound energy densities

Measurement of net specific energy (J g⁻¹) upon sonication was calculated from three parameters, i.e., electrical power consumption, sonication duration and volume of milk fat as (power drawn × sonication time)/volume of AMF. In this study, since the sonication time is quite short (5 s) and sonication treatment was carried out using the small double-jacketed glass vessel, it is assumed that the heat lost was negligible in such a laboratory scale reactor. Nevertheless, heat losses need to be taken in account if large-scale vessel is used (Son, Lim, Khim, Kim, & Ashokkumar, 2012).

2.5. Measurement of residual CO₂ content

CO₂ retention level in solidifying AMF after storage for 48 h at either 5 or 25 °C was measured using the titration method described by Jakobsen and Bertelsen (2006). AMF sample (approximately 2 g) was transferred into a Buchner flask containing 5 mL 0.5 M H₂SO₄ connected to another flask containing a standardised 0.1 M Ba(OH)₂ solution using a neoprene tubing. In this system, the standardised Ba(OH)₂ reacted with evolved CO₂, leading to formation of precipitated BaCO₃. After equilibrating for 18–24 h, titration of residual amount of Ba(OH)₂ using a standard HCl solution (0.1 M) was carried out with phenolphthalein as the indicator.

2.6. Melting properties

Thermal properties of AMF were measured by Differential Scanning Calorimetry (DSC1 STAR^e System, Mettler-Toledo, Schwerzenbach, Switzerland), calibrated using an indium standard (melting point = 156.66 °C, ΔH melting = 28.41 J g⁻¹). Approximately 10–15 mg of AMF was placed in a 40 μL aluminium pan and hermetically sealed (an empty pan was used as a reference). The DSC pan was heated from either 5 °C or 25 °C–60 °C at a heating rate of 5 °C min⁻¹. From the DSC melting curve obtained, endpoint of melting temperatures ($T_{M-endset}$) and melting enthalpy (ΔH_M) were calculated using STAR^e Excellence Software (Mettler-Toledo, Schwerzenbach, Switzerland). The $T_{M-endset}$ is defined as the intersectional point between the baseline and extrapolated leading edge of the signal of final heat absorption. Melting enthalpy was measured by integrating the peak area which starts from the onset to the endset points of thermal transition. STAR^e Excellence Software (Mettler-Toledo, Schwerzenbach, Switzerland) was used to analyse thermographs. All measurements were performed at least in duplicate.

2.7. Microstructure

Polarised light microscopy (PLM) was used to observe nucleation and growth of fat crystals. Pre-warming of microscopic accessories (microscopic slide, cover slip and pipette tip) were done prior to sampling at 28 °C. Fat sample (10 μL of liquid AMF) was placed onto the pre-warmed microscope slide, which was previously positioned in a sample chamber connected to a temperature controller (PE-95 Linkpad; Linkam Scientific Instruments, Surrey, UK). Visualisation of AMF structure was done with a CX41 microscope (Olympus, Tokyo, Japan) at 4× magnification.

2.8. Texture analysis

Texture analysis was performed with a TA.TX2 plus texture analyser (Stable Micro System, Surrey, UK) to determine hardness of the AMF (Wright, Scanlon, Hartel, & Marangoni, 2001). The 2 mm cylindrical probe was programmed to travel at a 1 mm s⁻¹ test speed for a distance of 10 mm in a compression test mode. Hardness of each AMF sample was analysed by this compression test for at least 5 replicates.

2.9. Peroxide values

Primary oxidation products were analysed on the basis of peroxide value adopted from AOAC Official Method 965.33 (AOAC, 1997). In this iodometric test, sample (5.00 g) was transferred to an Erlenmeyer flask, followed by addition of a mixture of acetic acid and chloroform (30 mL). The solution was shaken and saturated potassium iodide (0.5 mL) was added. Vigorous swirling was performed for exactly 1 min. Distilled water (30 mL) was added. Starch solution (1%) as an indicator was added (0.5 mL) and the solution was shaken vigorously. Titration was carried out with 0.001 M sodium thiosulphate (n_1) until the blue colour is discharged. Determination of titrated volume of blank titration (n_2) was undertaken under the same condition. PV was expressed as milliequivalents of active oxygen the quantity of peroxide contained in 1 kg of sample. Calculation of PV (mEq of peroxide kg of AMF⁻¹) was as follows: $[1000 \times (n_1 - n_2) \times \text{molarity of sodium thiosulfate}] / \text{sample weight in g}$.

2.10. Statistical analysis

All experimental treatments were done in triplicate with all measurements done at least in duplicate. The statistical package MINITAB[®] Released 16 (Minitab Co., Pennsylvania, US) was employed to analyse the data. Two-way ANOVA and Tukey's LSD were employed to determine significant differences of treatment means at $P < 0.05$.

3. Results and discussion

3.1. Absorption of CO₂ and specific ultrasound energy values

The equilibrium dissolved CO₂ concentration in molten AMF at 35 °C and its residual content after ultrasound treatment and storage at 25 and 5 °C for 48 h are presented in Table 1. CO₂ was highly solubilised in liquid AMF at 35 °C after 24 h of equilibrium. Solubilised CO₂ concentration increased with increasing amount of CO₂ added. Solubilities for CO₂ were in ranges of 417–447, 772–813, and 1525–1575 ppm, corresponding to CO₂ addition levels of 500, 1000 and 2000 ppm, respectively. After sonication and storage, CO₂ content in AMF was significantly reduced. Dissolved CO₂ concentrations retained in the 500, 1000 and 2000 ppm CO₂ treatments were 332–337, 398–675, and 530–901 ppm, respectively. CO₂ retention levels in combined CO₂ + ultrasound-treated AMF were much lower than in carbonated AMF alone (Table 1), particularly at the highest level of CO₂ addition. At the same added CO₂ levels and storage temperatures, the amount of CO₂ retained in non-sonicated AMF after 1000 and 2000 ppm CO₂ addition were 637–823 and 1200–1379 ppm, respectively. The decrease of CO₂ content in sonicated samples might be explained by a combination of the general “degassing” effect of sonication, plus the fact that CO₂ was able to escape from the open vessel during sonication, even though the sonication time was very short (5 s). Since the effect of degassing is prominent, sonication in a closed system would have little impact on retaining CO₂ in the sonicated AMF.

Table 1
Absorption/retention of CO₂ in AMF and US energy densities yielded.^a

Initial CO ₂ conc. (ppm)	US amplitude (%)	Adsorbed CO ₂ conc. (ppm)	CO ₂ retention at		US energy densities yielded (J g ⁻¹)
			25 °C, 48 h (ppm)	5 °C, 48 h (ppm)	
0	0	—	—	—	n/a
1000	0	953	823	637	n/a
2000	0	1887	1379	1200	n/a
0	10	222	138	139	0.11 ± 0.00
500	10	447	337	352	0.06 ± 0.02
1000	10	803	646	648	0.07 ± 0.00
2000	10	1575	530	825	0.07 ± 0.01
0	30	222	151	134	0.82 ± 0.01
500	30	417	332	296	0.74 ± 0.03
1000	30	772	398	499	0.66 ± 0.03
2000	30	1525	544	842	0.57 ± 0.04
0	50	222	136	131	1.93 ± 0.04
500	50	427	345	377	1.78 ± 0.04
1000	50	813	675	628	1.67 ± 0.02
2000	50	1535	725	901	1.50 ± 0.01

^a The CO₂ content of original AMF (non-carbonated/non-sonicated sample) was 222 ppm; adsorbed CO₂ concentration was at 35 °C, 24 h; n/a, not applicable.

The sonication energy densities achieved in this study varied from 0.06 to 1.93 J g⁻¹ depending on levels of applied power amplitude (Table 1) and are significantly lower than those reported in some previous studies on sonication of AMF (Frydenberg et al., 2013; Martini et al., 2008). At these levels, it is likely that the results of ultrasound treatment can be ascribed to a mixture of both stable and transient cavitation effects (Arends et al., 2003). The local temperature around the sonication probe was not measured in this study. Since the sonication time was extremely short (5 s) and the yielded sonication energy densities were very small, it is assumed that local heating was minimal. In this study, at the same level of applied power, the energy density fell significantly with increasing CO₂ concentration. For example, sonication energy density was 1.50 J g⁻¹ in 2000 ppm carbonated AMF as compared with 1.93 J g⁻¹ for non-carbonated AMF sonicated at 50% amplitude (Table 1). Less power was drawn in carbonated AMF at constant amplitude, implying that the gas content in AMF greatly impacted on the intensity of sonication. This is in agreement with the observation of Sivasankar et al. (2007) who reported that intensity of cavitation was less in high gas environments.

3.2. Melting properties

Melting profiles and melting properties of fats typically reflect the chemical composition of triacylglycerols, fat crystal size and amount of crystalline phase. In this study, the thermal properties of carbonated AMF were analysed after sonication at 28 °C, then cooled to either 25 °C ($\Delta T = 3$ °C) or 5 °C ($\Delta T = 23$ °C) and maintained at the final temperature for 48 h.

DSC analysis showed that CO₂ concentration, ultrasound amplitude and their interaction had significant influences on AMF endset-melting temperatures and melting enthalpies ($P < 0.05$) (Table 2). The endset-melting temperature tended to decrease with more dissolved CO₂ at both conditions. It is speculated that this may be due faster melting of the higher proportion of smaller crystals present in carbonated AMF. Samples sonicated at 30% amplitude had lower melting temperatures than sonicated samples treated at 10 and 50% amplitudes. Similar trends were observed for both crystallisation conditions, indicating that there may be an optimum power level required for crystallisation enhancement by CO₂, above which other effects start to negate this synergy. All

Table 2
Effects of dissolved CO₂ and ultrasound on final melting temperature ($T_{M-endset}$) and melting enthalpy (ΔH_M) of AMF.^a

Initial CO ₂ concentration (ppm)	US amplitude (%)	Stored at 25 °C, 48 h		Stored at 5 °C, 48 h	
		$T_{M-endset}$ (°C)	ΔH_M (J g ⁻¹)	$T_{M-endset}$ (°C)	ΔH_M (J g ⁻¹)
0	0	43.7 ± 0.2 ^a	33.0 ± 1.1 ^b	38.5 ± 0.1 ^a	104.1 ± 3.6 ^a
1000	0	43.7 ± 0.0 ^a	31.8 ± 0.9 ^b	39.8 ± 1.0 ^a	110.3 ± 2.6 ^a
2000	0	43.4 ± 0.1 ^b	43.0 ± 1.0 ^a	40.4 ± 1.5 ^a	111.3 ± 6.6 ^a
0	10	43.8 ± 0.1 ^a	33.5 ± 1.6 ^b	41.2 ± 0.0 ^{cd}	93.4 ± 1.4 ^b
500	10	43.3 ± 0.2 ^{bc}	33.2 ± 1.5 ^b	41.2 ± 0.1 ^{cd}	104.9 ± 1.4 ^a
1000	10	43.0 ± 0.3 ^{cd}	29.6 ± 1.9 ^c	40.9 ± 0.1 ^e	106.5 ± 0.3 ^a
2000	10	42.8 ± 0.1 ^d	38.1 ± 1.3 ^a	40.4 ± 0.2 ^f	106.4 ± 0.5 ^a
0	30	42.1 ± 0.3 ^{fg}	26.2 ± 0.2 ^d	41.1 ± 0.1 ^{de}	94.3 ± 5.7 ^b
500	30	42.4 ± 0.1 ^{ef}	27.6 ± 0.8 ^d	40.5 ± 0.1 ^f	92.9 ± 4.7 ^{bc}
1000	30	42.0 ± 0.1 ^g	27.4 ± 0.6 ^d	39.6 ± 0.1 ^g	107.0 ± 1.4 ^a
2000	30	41.9 ± 0.3 ^g	27.5 ± 1.5 ^d	39.8 ± 0.3 ^g	105.9 ± 1.3 ^a
0	50	43.5 ± 0.4 ^{ab}	34.9 ± 1.3 ^b	42.2 ± 0.2 ^a	72.27 ± 3.9 ^d
500	50	42.5 ± 0.0 ^e	33.2 ± 0.2 ^b	41.9 ± 0.2 ^{ab}	89.86 ± 1.2 ^{bc}
1000	50	43.0 ± 0.1 ^{cd}	33.3 ± 0.4 ^b	41.4 ± 0.5 ^c	88.97 ± 1.6 ^c
2000	50	42.3 ± 0.1 ^{ef}	34.0 ± 1.1 ^b	41.6 ± 0.2 ^{bc}	88.74 ± 2.5 ^c

^a AMF treated with two regimes: isothermal crystallisation (at 28 °C) and non-isothermal crystallisation (cooling from 35 to 5 °C) and kept at 25 and 5 °C for 48 h, respectively. All data are mean values ± standard deviation; values within a column with the same superscript letter are not significantly different ($P = 0.05$).

samples crystallised upon cooling from 28 to 5 °C and showed a clear trend of higher melting enthalpy values with higher dissolved CO₂ concentrations. This was also apparent for samples sonicated at 10% amplitude and then crystallised isothermally at 25 °C. However, when sonicated at higher amplitudes (30 and 50%) and then crystallised isothermally, the discrepancy in melting enthalpy values between various CO₂ concentrations was negligible statistically ($P > 0.05$).

Generally, melting enthalpy is associated with the proportion of crystalline materials, while differences in melting profile can indicate differences in crystal size and crystalline packing (Sato, 2001; Suzuki et al., 2010). Fig. 1 illustrates melting profiles of AMF under both crystallisation conditions. The AMF cooled from 28 to 5 °C and

kept at 5 °C for 48 h was characterised by two major melting peaks at 5–23 °C and 23–42 °C, indicating melting of middle- (MMF) and high-melting point (HMF) triacylglycerol (TAG) fractions, respectively. Melting profiles of AMF isothermally crystallised at 25 °C showed a broad melting peak over 25–43 °C, which is ascribed to melting of high-melting point TAGs (Fig. 1D–F). In contrast to HMF peaks of AMF crystallised at 5 °C, the melting peaks of AMF solidified at 25 °C were shifted to lower temperatures (Fig. 1A–C).

Fig. 2 illustrates the percentage of solid fat of all samples over temperature range of 25–40 °C (full temperature range can be found in Supplementary material Fig. S1), which was calculated by integrating the melting peaks. The melting profiles of carbonated AMF sonicated at 30% amplitude (both 5 and 25 °C) and 10%

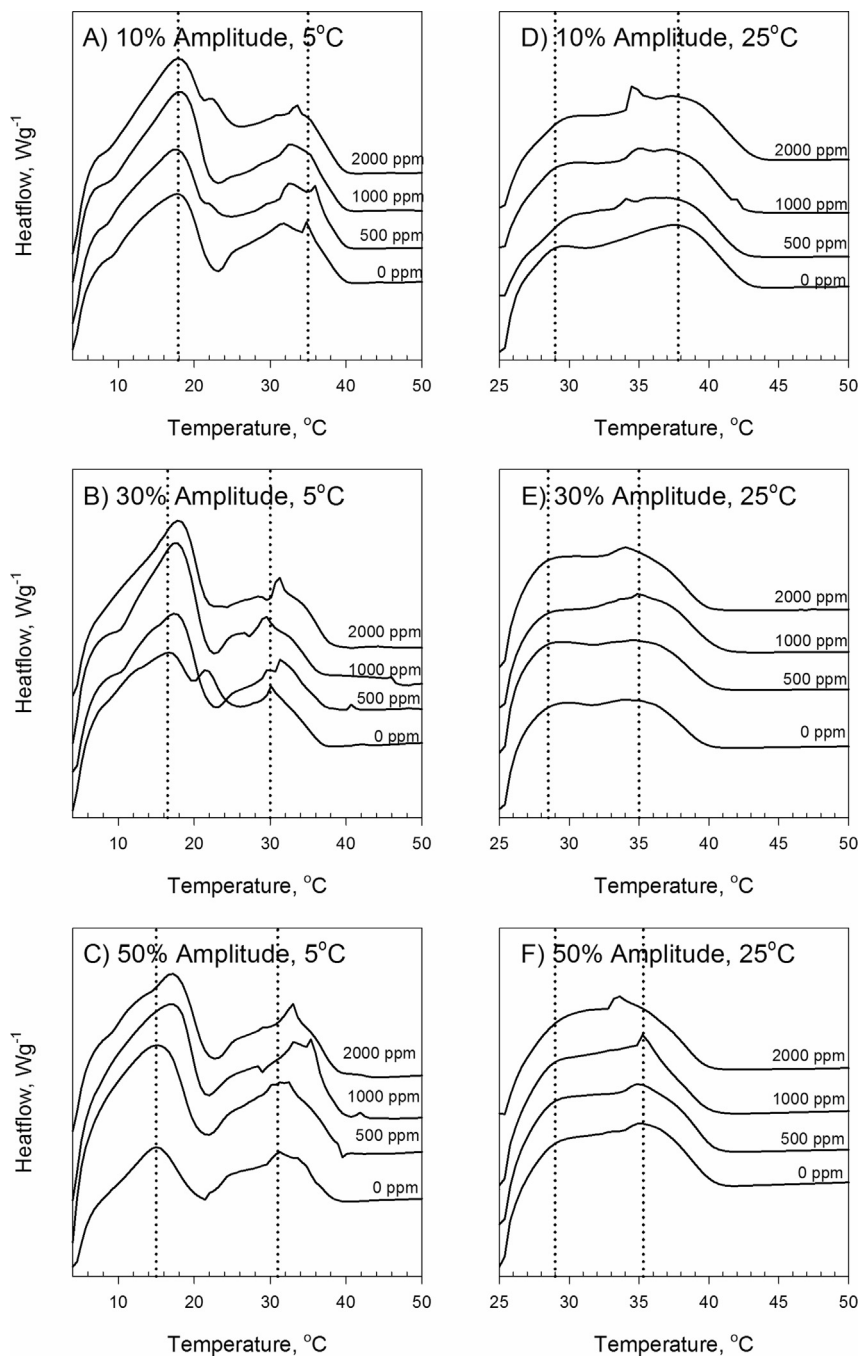


Fig. 1. Representative melting profiles of carbonated AMF (0–2000 ppm) sonicated at various power amplitudes (10, 30 and 50%) under cooling (A–C) and isothermal (D–F) crystallisation conditions.

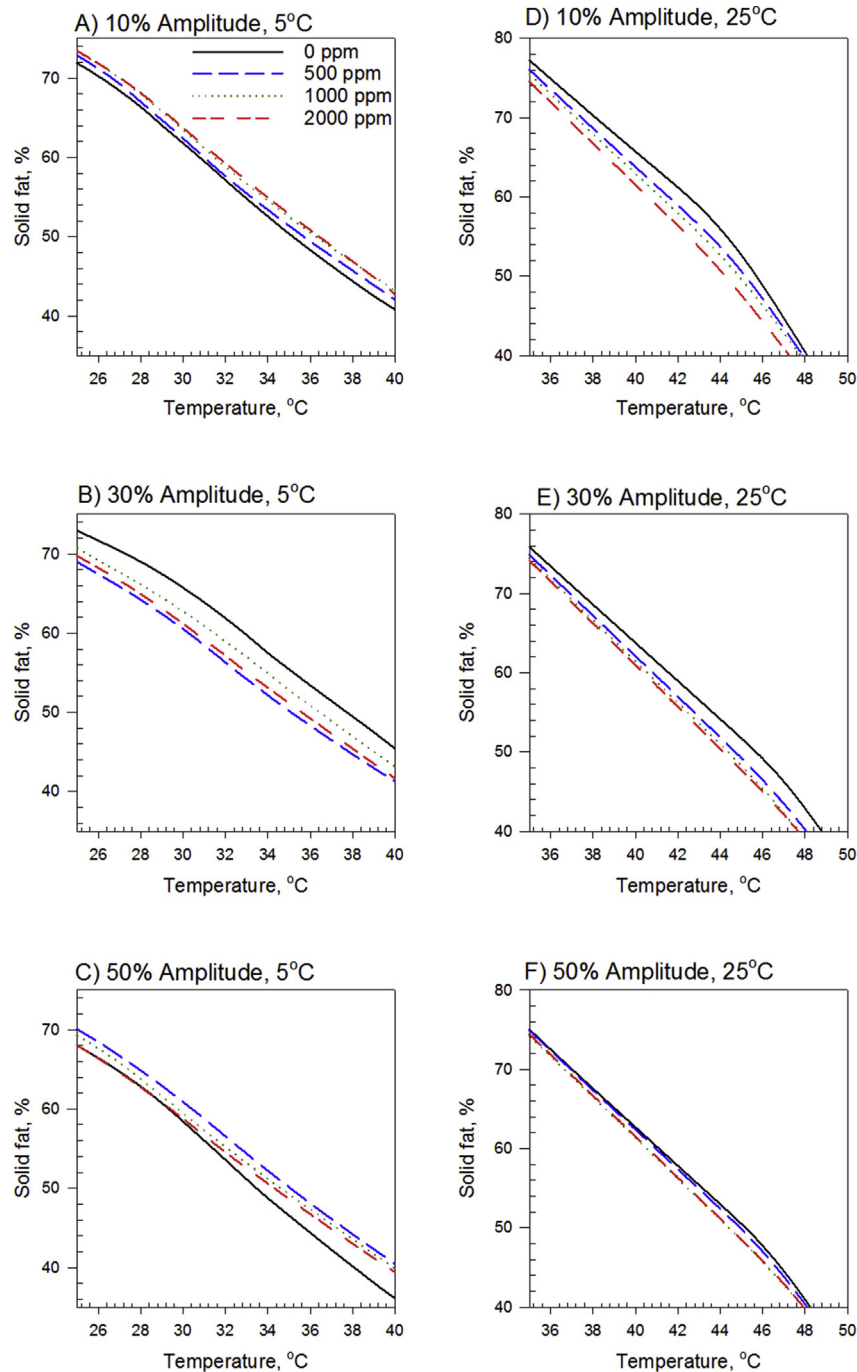


Fig. 2. Accumulative solid fat percentage over temperature range of 25–40 °C (as integrated from DSC melting curves) of carbonated AMF (0–2000 ppm) sonicated at 10, 30 and 50% amplitude under cooling (A–C) and isothermal (D–F) crystallisation conditions. Full solid fat percentage profile can be seen in [Supplementary material, Fig. S1](#).

amplitude at 25 °C tended to be steeper as compared with non-carbonated sonicated AMF (Fig. 2B,D,E). Suzuki et al. (2010) also reported similar behaviour of sonicated AMF (20 kHz for 10 s) at 22–28 °C in which sonicated AMF had a steeper melting profile than non-sonicated AMF. The remaining melting profiles (Fig. 2A,C,F) did not exhibit a clear tendency of steepness in melting behaviour of AMF.

Irrespective of CO₂ concentration, higher US amplitudes resulted in lower melting enthalpy values in samples stored at 5 °C. For samples kept at 25 °C, melting enthalpy of AMF sonicated at 30% amplitude was lower than those sonicated at 10 and 50% amplitudes. This is a further indication that the longer-term development

of the crystalline state and physical properties of AMF can be influenced by treatments at the nucleation phase as well as by subsequent storage conditions. In other studies, it was reported that there was only a slight discrepancy in solid fat content between non-sonicated and sonicated AMF after isothermal crystallisation (Suzuki et al., 2010). For crystallisation by cooling, Frydenberg et al. (2013) revealed that after 20 min of crystallisation at 5 °C, the amount of solid fat in sonicated AMF was less than in the control sample and at 14 days of storage, this difference in solid fat content was about 5%. In the present study, lower melting enthalpy values, which indicate lower content of solid fat, were associated with more intense sonication (Table 2). It is possible that

development of the crystal lattice is constrained with higher ultrasound power levels and that crystallisation of specific TAG species may become more selective (Frydenberg et al., 2013).

3.3. Microstructure

The microstructure of AMF under two crystallisation conditions is presented in Figs. 3 and 4. There was no apparent difference in crystal morphology, with spherulites predominating in all treatments. Fig. 3 shows PLM images of AMF crystals formed after 75 min of isothermal crystallisation at 28 °C immediately after sonicating, with or without CO₂ addition. The clear effect of sonication alone was to induce smaller crystals and larger numbers of crystals than in the untreated AMF, with this ultrasound result being enhanced at higher power levels. This effect of sonication on the crystallisation of milk fat is well established from previous studies (Frydenberg et al., 2013; Martini et al., 2008; Suzuki et al., 2010). At the highest amplitude applied (50%), fat crystals were not uniformly distributed but seemed to aggregate as clusters (Fig. 3).

In general, when applying ultrasound alone for sonocrystallisation, higher intensity results in more energy input in the system. Hence, more ultrasound-induced bubbles are generated to induce primary nucleation and crystallisation with resultant fat crystals appearing to be smaller and more uniform. In this study, if CO₂ had no influence and sonication effects dominated the system, at the constant amplitude it would be expected that fat crystals would be bigger and fewer numbers of crystals would be generated with increasing dissolved CO₂ concentration, due to the higher gas content suppressing ultrasound intensity. However, the use of CO₂ not only accelerated crystallisation but appeared to enhance the effects of ultrasound as discussed below.

Under isothermal crystallisation (Fig. 3), it was also apparent that the general effect of carbonation was to enhance the effects

of ultrasound treatment, with increasing CO₂ concentration causing smaller fat crystals and a denser fat crystal network at all levels of ultrasound amplitude. However, one interesting difference was that fat crystals appeared to be dispersed evenly in the presence of CO₂ at 50% amplitude, rather than partially aggregated at this amplitude with ultrasound alone. This might be explained by the differences in energy densities. That is, for any given applied power level, the energy density was reduced with increasing CO₂ concentration. Significant crystal aggregation was only observed after treatment with the highest energy density, which was the highest amplitude of sonication, without carbonation. The synergistic effects of carbonation and sonication in this crystallisation system are possibly due to the CO₂ molecules and/or gas microbubbles acting as impurities to promote nucleation.

For the non-isothermal system, visualisation of AMF microstructure during cooling from 28 to 5 °C at cooling rate of 0.5 °C min⁻¹ was undertaken immediately after sonication at 28 °C. Fig. 4 shows PLM images captured at 20 °C and 5 °C during the cooling period. Due to the effect of supercooling on crystal habit, smaller crystal sizes were formed during the cooling regime from 28 to 5 °C (Fig. 4). The combined CO₂ and ultrasound treatment of AMF in non-isothermal crystallisation also induced denser crystal fat network, compared with non-ultrasound treatment. For example, at the 20 °C sampling point, fat crystal network in carbonated and sonicated AMF were denser than those in AMF treated by sonication alone (Fig. 4A), indicating that dissolved CO₂ promoted induction of crystallisation upon cooling. However, this effect was not carried over to the end of the cooling procedure, by which time (at 5 °C) the microstructure of all treatments appeared to be quite similar (Fig. 4B). This suggests that, under these conditions, the cooling effect is stronger than the effect of ultrasound and/or carbonation.

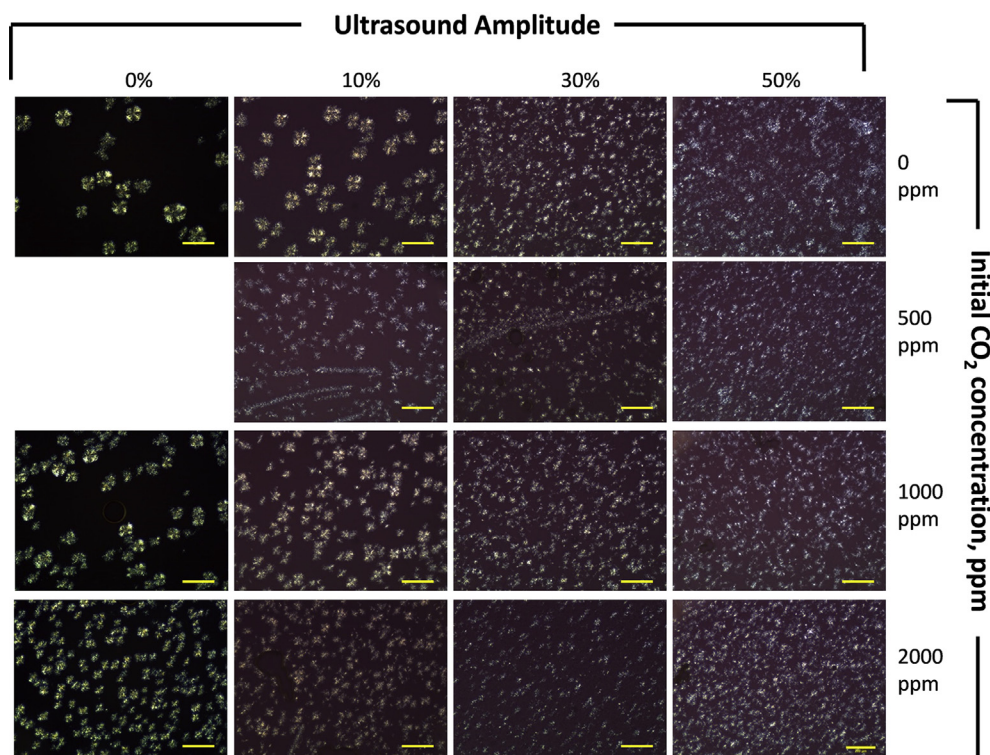


Fig. 3. Milk fat crystals formed upon solidifying at 28 °C for 75 min as visualised by polarised light microscopy. Effect of dissolved CO₂ alone, i.e., 0% amplitude applied, at 0 (original AMF), 1000 and 2000 ppm on AMF microstructure was also presented (left column). Scale bar represents 200 μm.

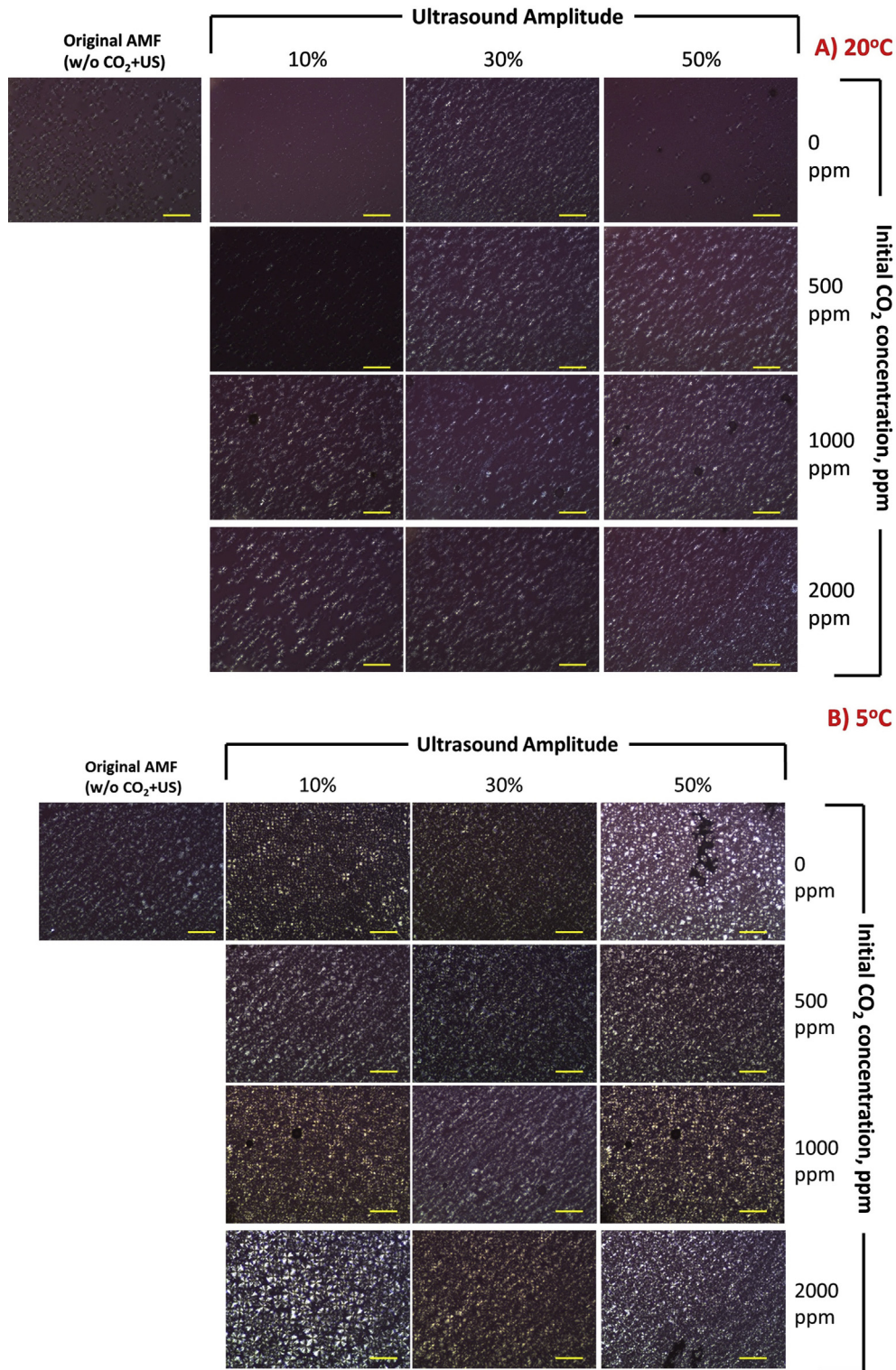


Fig. 4. Microscopic images of AMF under polarised light microscopy at 20 °C (A) and 5 °C (B) upon cooling from 28 to 5 °C showing the impact of different combinations of sonication and dissolved CO₂ on AMF microstructure. Scale bar represents 200 μm.

3.4. Textural properties

Hardness of AMF was examined after 48 h of storage at 25 and 5 °C. Regarding AMF crystallised at 25 °C, sonication alone at the weakest power had no effect on hardness but sonication at 30% and 50% amplitude significantly increased hardness after 2 days

(Table 3). There appeared to be little or no effect of CO₂ at the lowest sonication amplitude. At 30% amplitude, the highest concentration of CO₂ (2000 ppm) significantly increased hardness. At 50% amplitude, CO₂ at both 1000 and 2000 ppm also increased hardness. In general terms, for the 25 °C treatment, at higher sonication amplitudes and CO₂ concentrations, the apparent trend was for CO₂

Table 3
Hardness of the AMF under two crystallising conditions as functions of dissolved CO₂ concentrations and US amplitudes.^a

Initial CO ₂ conc. (ppm)	US amplitude (%)	Hardness (peak force, N)			
		Stored at 25 °C		Stored at 5 °C	
		Day 2	Day 9	Day 2	Day 9
0	10	0.22 ± 0.01 ^h	0.26 ± 3.65 ^h	27.42 ± 3.18 ^c	27.98 ± 2.06 ^f
500	10	0.27 ± 0.01 ^g	0.31 ± 2.90 ^h	29.43 ± 3.65 ^c	33.90 ± 2.14 ^{cde}
1000	10	0.26 ± 0.02 ^g	0.48 ± 6.97 ^g	29.20 ± 1.17 ^c	33.64 ± 3.86 ^{cde}
2000	10	0.29 ± 0.02 ^g	0.21 ± 11.11 ⁱ	28.01 ± 1.17 ^c	31.69 ± 1.14 ^e
0	30	0.56 ± 0.03 ^e	0.56 ± 1.75 ^e	35.23 ± 2.98 ^a	36.96 ± 2.02 ^{abc}
500	30	0.47 ± 0.01 ^f	0.47 ± 3.84 ^f	29.02 ± 1.35 ^c	32.81 ± 0.90 ^{de}
1000	30	0.56 ± 0.01 ^e	0.56 ± 0.01 ^{ef}	33.99 ± 1.47 ^{ab}	38.00 ± 1.66 ^{ab}
2000	30	0.78 ± 0.01 ^d	0.78 ± 0.01 ^d	30.90 ± 1.32 ^{bc}	36.43 ± 0.42 ^{bcd}
0	50	0.83 ± 0.03 ^c	0.83 ± 0.03 ^c	36.36 ± 0.46 ^a	40.41 ± 1.95 ^a
500	50	0.80 ± 0.05 ^d	0.80 ± 0.02 ^d	35.34 ± 0.94 ^a	38.89 ± 2.44 ^{ab}
1000	50	1.29 ± 0.02 ^b	1.29 ± 0.02 ^b	33.22 ± 2.44 ^{ab}	37.79 ± 2.41 ^{ab}
2000	50	1.80 ± 0.02 ^a	1.80 ± 0.02 ^a	33.52 ± 2.18 ^{ab}	37.33 ± 3.10 ^{abc}

^a Hardness values for non-carbonated/non-sonicated samples were 0.22 ± 0.01 and 0.26 ± 0.01 at days 2 and 9, respectively, when stored at 25 °C and 39.17 ± 0.96 and 44.60 ± 1.81 at days 2 and 9, respectively, when stored at 5 °C. All data are mean values ± standard deviation; ranges for coefficients variation were: 25 °C, day 2, 0.97–8.33%; 25 °C, day 9, 0.41–11.11%; 5 °C, day 2, 1.26–12.40%; 5 °C, day 9, 1.15–11.46%. Values within a column with the same superscript letter are not significantly different ($P = 0.05$).

to enhance hardness development caused by sonication, with the hardest texture being recorded for the highest sonication amplitude combined with the highest concentration of CO₂. However, at 25 °C there was generally no further change in hardness in the control or any treated sample when measured again at Day 9 (Table 3). Improvement in hardness of AMF and other lipids under sonication treatment has been reported in previous studies (Martini, 2013; Martini et al., 2008). Smaller crystal size and higher amount of fat crystals induced by ultrasound irradiation strengthen the fat crystal network during isothermal crystallisation.

When AMF was subjected to non-isothermal crystallisation by cooling from 28 to 5 °C, a quite different textural behaviour was observed. The most obvious difference is that these samples were all much harder (28–44 N) compared with those stored at 25 °C (0.2–1.8 N), regardless of treatment. There was also a marked contrast to the isothermal samples in terms of treatment effects, in that all cooled samples treated with ultrasound and/or CO₂ were softer than the control (Table 3). Similar effects were found by Frydenberg et al. (2013), who reported that hardness of sonicated AMF (5 s, 17.5 J mL⁻¹) at 22, 26 and 30 °C were all softer than control AMF after storage at 5 °C for 7 or 14 days.

For sonication alone, hardness increased with increasing amplitude, even though these values were all softer than the

control, a trend which is similar in some respects to that seen in isothermal samples (Table 3). However, the enhancement effect of CO₂ that was evident in some isothermal samples was not apparent in the cooled samples; indeed, other than the control samples, the hardest textures were all obtained by sonication without carbonation. To some extent, it can be seen that these contrasting effects of crystallisation conditions on texture mirror those seen in microstructure (Figs. 3 and 4).

In contrast to the isothermal samples, hardness of all cooled samples continued to increase from 2 to 9 days. It is speculated that this alteration in hardness most likely relates to polymorphic transition of TAGs rather than changes in the amount of crystalline materials. It has previously been reported that solid fat content in sonicated AMF remained the same after 1 h of crystallisation at 5 °C until 14 days of storage (Frydenberg et al., 2013).

3.5. Peroxide values

Presence of primary oxidation products in the AMF samples was measured by PVs (mEq peroxide kg⁻¹ fat). Fig. 5 represents the PV values of carbonated AMF without sonication. The PV of original AMF as reported by the manufacturer was below 0.01. At the beginning of storage duration (day 2), the initial PV of AMF stored at

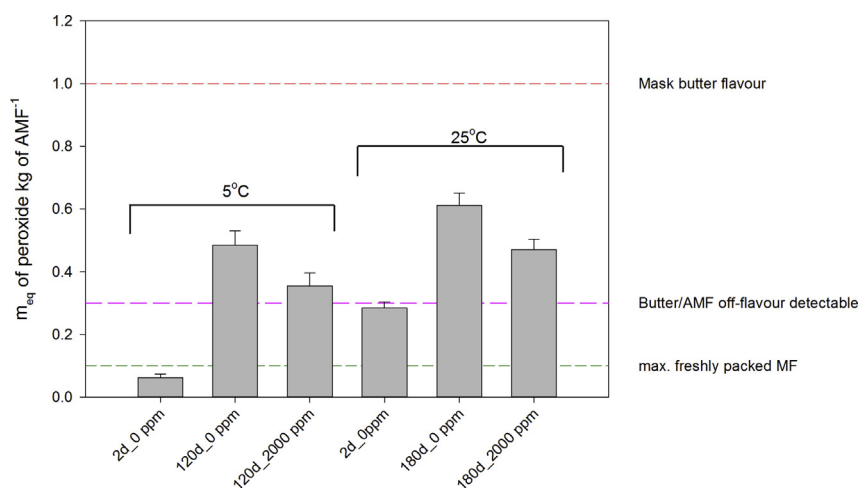


Fig. 5. Effect of carbonation at 2000 ppm on peroxide values (PVs) of AMF after 2 days (2 d), 4 months (120 d) and 6 months (180 d) storage at either 5 or 25 °C. Reference lines at 0.1, 0.3 and 1.0 PVs are standard values (mEq peroxide kg⁻¹ fat) used in dairy industry practice.

5 °C (0.062 ± 0.01 mEq peroxide kg^{-1} fat) was below the maximum level of PV permitted for anhydrous milk fat (0.3 mEq peroxide kg^{-1} fat) according to Codex Alimentarius (FAO/WHO, 2011). The PV of AMF increased almost 8-fold (0.484) upon storage at 5 °C for 4 months. When CO_2 was dissolved into the AMF at concentration of 2000 ppm, the PV of AMF was reduced to 0.355, which was just slightly above the threshold of off-flavour detectable (0.3 mEq peroxide kg^{-1} fat). A similar tendency was noted for samples stored at accelerated temperature (25 °C). Initial PV of AMF stored at 25 °C (0.284 ± 0.02 mEq peroxide kg^{-1} fat) was comparable with a previous study on oxidation of AMF (0.225 – 0.314 mEq peroxide kg^{-1} fat) (Keogh & Higgins, 1986). After 6 months of storage at 25 °C PV of carbonated AMF (2000 ppm) was also increased (0.470 ± 0.03 mEq peroxide kg^{-1} fat) but remarkably lower than that of non-carbonated AMF (0.612 ± 0.03 mEq peroxide kg^{-1} fat). The lower PVs of carbonated AMF at both temperatures indicate that formation of primary oxidation products has been delayed. Effectiveness of CO_2 in maintaining oxidative stability in fully refined rapeseed oil was also reported for gas blanket and flushing carbonation (Sionek et al., 2013). In addition, it was reported that CO_2 is more effective than nitrogen in inhibiting oxidative changes due to its higher solubility in edible oils, thus higher oxygen content can be displaced (Sionek et al., 2013). Our previous study also shows that CO_2 is highly soluble in AMF at 2536, 1648 and 164 mg CO_2 $\text{kg fat}^{-1} \text{atm}^{-1}$ at 35, 23.5 and 4 °C (Truong et al., 2017b). Truong, Palmer, Bansal, and Bhandari (2018) also reported residual

CO_2 content in butter grains (after churning of dairy cream) within the range of 888–958 ppm upon carbonation at 1000–2000 ppm. Compared with PV of nitrogen sparged AMF (100–140 kPa) in the literature (0.548 mEq peroxide kg^{-1} fat) (Keogh & Higgins, 1986), our result on PV of carbonated AMF (2000 ppm) was also lower (0.470 ± 0.03 mEq peroxide kg^{-1} fat) at the same storage temperature (25 °C) and time (6 months). In this study, the PV of carbonated AMF kept at room temperature (25 °C) after 6 months of storage is comparable to that of non-carbonated AMF stored at refrigerated AMF for 4 months. This demonstrates a pronounced impact of CO_2 in delaying lipid oxidation in AMF without sonication.

Effectiveness of carbonation on preventing oxidation changes in sonicated AMF is illustrated in Fig. 6. All influential factors such as storage temperature, storage time, US amplitude and CO_2 concentration had a significant impact on PVs of AMF ($P < 0.01$). Interactions between storage time \times storage day, storage day \times CO_2 concentration were also found ($P < 0.01$). Mean PVs of samples kept of 25 °C (0.377 mEq peroxide kg^{-1} fat) were significantly higher than those stored at refrigerated temperature (5 °C; 0.280 mEq peroxide kg^{-1} fat). This is in agreement with previous studies that rate of oxidation in AMF and butter is a function of temperature within range of -10 to 50 °C (Hamm, Hammond, & Hotchkis, 1968; Krause, Miracle, Sanders, Dean, & Drake, 2008). There was an increase in PVs with storage duration up to 90 d for all treatments, indicating the usage of oxygen dissolved in AMF for the lipid

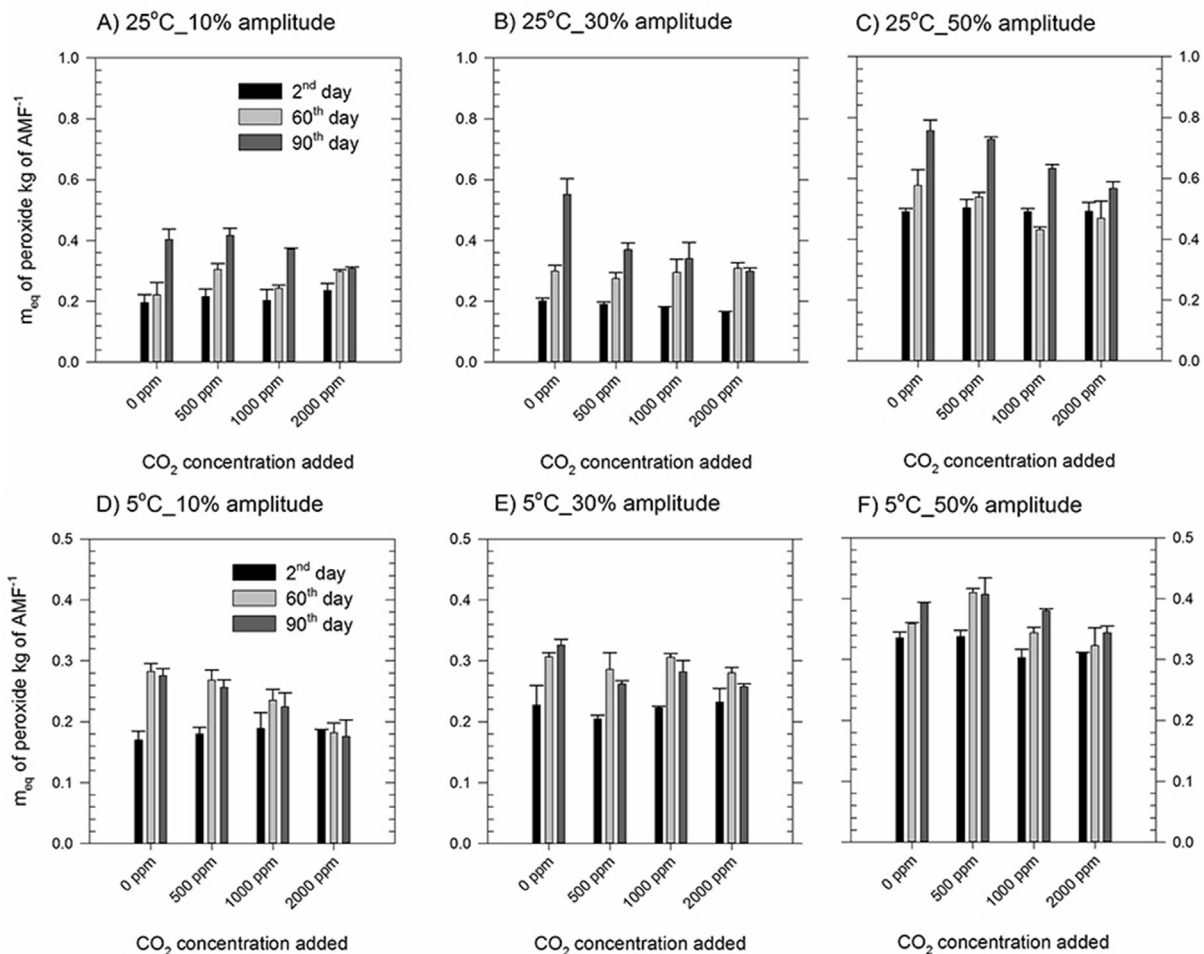


Fig. 6. The influence of carbonation at various levels (0, 500, 1000, 2000 ppm) on peroxide values (PVs) of AMF sonicated at three amplitudes (10, 30, and 50%) and then kept at room (25 °C; A–C) and refrigerated (5 °C; D–F) temperature up to 90 d.

oxidation reaction. Previous studies also reported the increasing trend of PVs with storage time up to 8 months at 25 °C in AMF (Keogh & Higgins, 1986) and 18 months in frozen and refrigerated butter (Krause et al., 2008).

In this study, intensity of ultrasound had a remarkable effect on PVs of sonicated AMF. At the same storage temperature, the formation of peroxides is accelerated with application of 50% amplitude. From the beginning of storage duration, the AMF sonicated at 50% amplitude had higher PVs whereas similar range of PVs was found between 10% and 30% amplitudes (Fig. 6). For instance, at day 2, PV values of non-carbonated AMF sonicated at 50% amplitude (0 ppm of CO₂) were significantly higher than those of non-treated AMF stored at 25 °C (0.49 ± 0.01 versus 0.284 ± 0.02 mEq peroxide kg⁻¹ fat; $P < 0.05$) and 5 °C (0.336 ± 0.01 versus 0.062 ± 0.01 mEq peroxide kg⁻¹ fat; $P < 0.05$). The PVs kept increasing with storage time at all levels of US amplitudes (Fig. 6). It should be stressed that the lipid oxidation accelerated with time regardless of treatment methods (no treatment, carbonation only, sonication only and combined carbonation + sonication) as shown in Figs. 5 and 6. After being stored at 25 °C for 90 d, the PV value of AMF sonicated at 50% amplitude having no carbonation increased to 0.76 ± 0.05 mEq peroxide kg⁻¹ fat, which was remarkably higher than the PV value of non-treated AMF (0.612 ± 0.03 mEq peroxide kg⁻¹ fat) stored at the same temperature for longer duration (180 d; Fig. 5). This study showed that, specific energy input as low as 1.50 J g⁻¹ (50% US amplitude; Table 1) can trigger the generation of free radicals in sonicated AMF, propagating the oxidative reactions, as measured by PV (Fig. 6). Previous studies also reported dependence of lipid oxidation in edible fats/oils on specific conditions of sonication and type of products. For example, investigation of oxidative stability of sonicated soybean oil and low saturated shortening under sonication condition of 10 s, 100 W power, 3.2 diameter tip showed no change in PV of the samples kept at 25 °C for 190 d (Martini, 2013). Sonication of sunflower oil for 5 min at 20 kHz also showed no detrimental impact on its oxidative stability (Patrick, Blindt, & Janssen, 2004). However, application of severe ultrasonic regime (20 kHz probe, 150 W for 0.5–30 min) induced lipid oxidation in sunflower oil (Chemat et al., 2004). Similar observations were reported for dairy products. Oxidation-derived volatile compounds were present in raw and pasteurised milks after subjected to ultrasonication with high energy inputs (187–240 kJ kg⁻¹) (Chouliara, Georgogianni, Kanellou, & Kontominas, 2010; Riener, Noci, Cronin, Morgan, & Lyng, 2009) whereas applying higher energy input (390 kJ kg⁻¹) did not generate lipid oxidative volatile compounds in fresh Cheddar whey (Torkamani, Juliano, Ajlouni, & Singh, 2014).

As previously discussed, carbonation delays the formation of oxidation products in non-sonicated AMF up to 6 months of storage (Fig. 5). Similar tendency was observed when addition of CO₂ is applied to AMF prior to ultrasonication. When CO₂ was dissolved in the AMF at high concentration (1000 and 2000 ppm), the residual CO₂ concentration after sonication and storage for 48 h were 398–725 ppm and 499–901 ppm at 25 and 5 °C, respectively (Table 1). These concentrations appeared sufficient to protect US-treated AMF against lipid oxidation reflected by lower PVs at the same storage temperature and duration (Fig. 6). At this point, it is still unclear whether the formation of free radicals is also prevented by the presence of CO₂ prior sonication or the effect was post-sonication. Further studies, which measure quantity of free radicals formed in carbonated AMF prior- and post-sonication, are therefore recommended. Low concentration of added CO₂ (500 ppm), which had residual CO₂ content in range of 345–377 ppm (Table 1), did not improve the oxidative stability of sonicated AMF. There was no statistically significant difference in PV between non-CO₂ and 500 ppm CO₂-added AMF ($P > 0.01$).

Volatile lipid oxidation products are associated with secondary lipid oxidation and responsible for undesirable flavours in food products. In this study, an attempt was made to characterise headspace volatile compounds of aldehydes (hexanal and propanal) and ketones (propanone, 2-butanone and 2-heptanone) in all samples up to 90 d using solid phase microextraction (SPME) and gas chromatography-mass spectrometry (GC–MS) techniques. In general, oxidation volatiles, particularly hexanal and propanal, are likely to accelerate with higher storage temperature, longer storage durations, and higher applied US amplitudes (data not shown). Panseri, Soncin, Chiesa, and Biondi (2011) also reported similar observation that hexanal increased constantly in butter stored at 4 °C for 180 d. However, it was observed that residual CO₂ in AMF samples modified the sample composition and induced variations of headspace volatile abundance. This agrees with a previous report on carbonated drinks in which CO₂ was found to increase the volatility parameters (gas-to-product-partition coefficient) of some headspace component. As a result, carbonation resulted in higher amounts of aroma compounds being released in both in vitro and in vivo conditions (Saint-Eve et al., 2009). At this point, the effect of residual CO₂ on secondary oxidation, as reflected by oxidation headspace volatile compounds, is still unclear due to possible interference of sample matrix.

4. Conclusions

Our previous research demonstrated the effect of dissolved CO₂ at low pressure on crystallisation, microstructural and textural properties of AMF (Truong et al., 2017a). This study has shown that, depending on crystallisation conditions, the effects of CO₂ mirror those of high-intensity, low frequency ultrasound and that carbonation can be used to enhance the effects of sonication in accelerating nucleation, reducing crystal size, increasing crystal number and increasing degree of crystallisation of AMF. Furthermore, under selected crystallisation regimes, carbonation can enhance the effects of ultrasound in modulating the hardness of AMF. This study also demonstrates that addition of CO₂ is beneficial to oxidative stability of US-treated AMF. The increase in PVs was less with increasing dissolved CO₂ concentrations regardless of storage conditions and ultrasound intensities treated. Taken together, thanks to multiple effects of addition of CO₂ in AMF, CO₂ can be considered as a potent method to modify fat crystals size and size distribution as well as minimise lipid oxidation in sonicated AMF and possibly can be applied to other edible fats and oils and fat containing liquid or solid food products.

To the best of our knowledge, this is the first time CO₂ has been reported to enhance the sonocrystallisation of any lipid material. Indeed, apart from a study by Zhang et al. (2003), which showed that ice nucleation was highly accelerated when water was supersaturated with air bubbles before sonication (Zhang et al., 2003) and our study on CO₂-enhanced crystallisation of alpha-lactose monohydrate (Xun et al., 2017) there appear to be no other published reports on gas-enhanced sonocrystallisation in edible fats. This process may be of interest industrially to improve the yield of sonocrystallisation processes or to provide a means to sonicate at lower energy densities, thereby using less power and reducing the risk of free radical generation. For edible fats and oils, provided that sensory acceptance is maintained, the use of CO₂ in this way may also help to prevent the development of oxidative rancidity by displacing dissolved oxygen.

Acknowledgements

This research was supported under Australian Research Council's Industrial Transformation Research Program (ITRP) funding

scheme (project number IH120100005). The ARC Dairy Innovation Hub is a collaboration between The University of Melbourne, The University of Queensland and Dairy Innovation Australia Ltd.

Appendix A. Supplementary data

Supplementary data to this article can be found online at <https://doi.org/10.1016/j.idairyj.2019.02.001>.

References

- Adhikari, B., Truong, T., Bansal, N., & Bhandari, B. (2018). Influence of gas addition on crystallisation behaviour of lactose from supersaturated solution. *Food and Bioprocess Processing*, *109*, 86–97.
- AOAC. (1997). *Official methods of analysis of AOAC International*. Gaithersburg, MD, USA: AOAC International.
- Arends, B. J., Blint, R. A., Janssen, J., & Patrick, M. (2003). US Patent No. 6,630,185 B2. Retrieved from: <https://patents.google.com/patent/US6630185>.
- Chemat, F., Grondin, I., Costes, P., Moutoussamy, L., Shum, A., Sing, A. S. C., et al. (2004). High power ultrasound effects on lipid oxidation of refined sunflower oil. *Ultrasonics Sonochemistry*, *11*, 281–285.
- Chouliara, E., Georgogianni, K. G., Kanellopoulou, N., & Kontominas, M. G. (2010). Effect of ultrasonication on microbiological, chemical and sensory properties of raw, thermized and pasteurized milk. *International Dairy Journal*, *20*, 307–313.
- FAO/WHO. (2011). *Codex alimentarius milk and milk products. Codex Standard for Milk fat products CODEX STAN 280-1973*. Rome, Italy: Codex alimentarius.
- Frydenberg, R. P., Hammershoj, M., Andersen, U., & Wiking, L. (2013). Ultrasonication affects crystallization mechanisms and kinetics of anhydrous milk fat. *Crystal Growth & Design*, *13*, 5375–5382.
- Hamm, D. L., Hammond, E. G., & Hotchkis, D. K. (1968). Effect of temperature on rate of autoxidation of milk fat. *Journal of Dairy Science*, *51*, 483–491.
- Han, L. J., Li, L., Li, B., Zhao, L., Liu, G. Q., Liu, X. Q., et al. (2014). Effect of high pressure microfluidization on the crystallization behavior of palm stearin – palm olein blends. *Molecules*, *19*, 5348–5359.
- Higaki, K., Ueno, S., Koyano, T., & Sato, K. (2001). Effects of ultrasonic irradiation on crystallization behavior of tripalmitoylglycerol and cocoa butter. *Journal of the American Oil Chemists Society*, *78*, 513–518.
- Jakobsen, M., & Bertelsen, G. (2006). Solubility of carbon dioxide in fat and muscle tissue. *Journal of Muscle Foods*, *17*, 9–19.
- Keogh, M. K., & Higgins, A. C. (1986). Anhydrous milk-fat 1. Oxidative stability aspects. *Irish Journal of Food Science & Technology*, *10*, 11–22.
- Krause, A. J., Miracle, R. E., Sanders, T. H., Dean, L. L., & Drake, M. A. (2008). The effect of refrigerated and frozen storage on butter flavor and texture. *Journal of Dairy Science*, *91*, 455–465.
- Lopez, C., Lavigne, F., Lesieur, P., Keller, G., & Ollivon, M. (2001). Thermal and structural behavior of anhydrous milk fat. 2. Crystalline forms obtained by slow cooling. *Journal of Dairy Science*, *84*, 2402–2412.
- Marangoni, A. G., Acevedo, N., Maleky, F., Co, E., Peyronel, F., Mazzanti, G., et al. (2012). Structure and functionality of edible fats. *Soft Matter*, *8*, 1275–1300.
- Marchesini, G., Balzan, S., Montemurro, F., Fasolato, L., Andrighetto, I., Segato, S., et al. (2012). Effect of ultrasound alone or ultrasound coupled with CO₂ on the chemical composition, cheese-making properties and sensory traits of raw milk. *Innovative Food Science & Emerging Technologies*, *16*, 391–397.
- Martini, S. (2013). *Sonocrystallization of fats*. New York, NY, USA: Springer-Verlag.
- Martini, S., Suzuki, A. H., & Hartel, R. W. (2008). Effect of high intensity ultrasound on crystallization behavior of anhydrous milk fat. *Journal of the American Oil Chemists Society*, *85*, 621–628.
- Panseri, S., Soncin, S., Chiesa, L. M., & Biondi, P. A. (2011). A headspace solid-phase microextraction gas-chromatographic mass-spectrometric method (HS-SPME-GC/MS) to quantify hexanal in butter during storage as marker of lipid oxidation. *Food Chemistry*, *127*, 886–889.
- Patrick, M., Blindt, R., & Janssen, J. (2004). The effect of ultrasonic intensity on the crystal structure of palm oil. *Ultrasonics Sonochemistry*, *11*, 251–255.
- Perry, R. H., & Green, D. W. (2007). *Perry's chemical engineers' handbook*. London, UK: McGraw-Hill.
- Riener, J., Noci, F., Cronin, D. A., Morgan, D. J., & Lyng, J. G. (2009). Characterisation of volatile compounds generated in milk by high intensity ultrasound. *International Dairy Journal*, *19*, 269–272.
- Saint-Eve, A., Deleris, I., Aubin, E., Semon, E., Feron, G., Rabillier, J. M., et al. (2009). Influence of composition (CO₂ and sugar) on aroma release and perception of mint-flavored carbonated beverages. *Journal of Agricultural and Food Chemistry*, *57*, 5891–5898.
- Sato, K. (2001). Crystallization behaviour of fats and lipids – a review. *Chemical Engineering Science*, *56*, 2255–2265.
- Sionek, B., Krygier, K., Ukalski, K., Ukalska, J., & Amarowicz, R. (2013). The influence of nitrogen and carbon dioxide on the oxidative stability of fully refined rapeseed oil. *European Journal of Lipid Science and Technology*, *115*, 1426–1433.
- Sivasankar, T., Paunikar, A. W., & Moholkar, V. S. (2007). Mechanistic approach to enhancement of the yield of a sonochemical reaction. *Aiche Journal*, *53*, 1132–1143.
- Smith, K. W., Bhagga, K., Talbot, G., & van Malssen, K. F. (2011). Crystallization of fats: Influence of minor components and additives. *Journal of the American Oil Chemists Society*, *88*, 1085–1101.
- Son, Y., Lim, M., Khim, J., Kim, L.-H., & Ashokkumar, M. (2012). Comparison of calorimetric energy and cavitation energy for the removal of bisphenol-A: The effects of frequency and liquid height. *Chemical Engineering Journal*, *183*, 39–45.
- Suzuki, A. H., Lee, J., Padilla, S. G., & Martini, S. (2010). Altering functional properties of fats using power ultrasound. *Journal of Food Science*, *75*, E208–E214.
- Torkamani, A. E., Juliano, P., Ajlouni, S., & Singh, T. K. (2014). Impact of ultrasound treatment on lipid oxidation of Cheddar cheese whey. *Ultrasonic Sonochemistry*, *21*, 951–957.
- Truong, T., Palmer, M., Bansal, N., & Bhandari, B. (2017a). Effect of solubilised carbon dioxide at low partial pressure on crystallisation behaviour, microstructure and texture of anhydrous milk fat. *Food Research International*, *95*, 82–90.
- Truong, T., Palmer, M., Bansal, N., & Bhandari, B. (2017b). Investigation of solubility of carbon dioxide in milk fat by lab-scale manometric method. *Food Chemistry*, *237*, 667–676.
- Truong, T., Palmer, M., Bansal, N., & Bhandari, B. (2018). Effects of dissolved carbon dioxide in fat phase of cream on manufacturing and physical properties of butter. *Journal of Food Engineering*, *226*, 9–21.
- Wright, A. J., Scanlon, M. G., Hartel, R. W., & Marangoni, A. G. (2001). Rheological properties of milkfat and butter. *Journal of Food Science*, *66*, 1056–1071.
- Xun, A., Truong, T., & Bhandari, B. (2017). Effect of carbonation of supersaturated lactose solution on crystallisation behaviour of alpha-lactose monohydrate. *Food Biophysics*, *12*, 52–59.
- Xu, B. G., Zhang, M., Bhandari, B., & Cheng, X. F. (2014). Influence of power ultrasound on ice nucleation of radish cylinders during ultrasound-assisted immersion freezing. *International Journal of Refrigeration*, *46*, 1–8.
- Zamanipoor, M. H., Dincer, T. D., Zisu, B., & Jayasena, V. (2013). Nucleation and growth rates of lactose as affected by ultrasound in aqueous solutions. *Dairy Science & Technology*, *93*, 595–604.
- Zhang, X., Inada, T., & Tezuka, A. (2003). Ultrasonic-induced nucleation of ice in water containing air bubbles. *Ultrasonics Sonochemistry*, *10*, 71–76.